



Distraction forces on the spine in early-onset scoliosis: A systematic review and meta-analysis of clinical and biomechanical literature

Justin V.C. Lemans^{a,*}, Sebastiaan P.J. Wijdicks^a, Ioannis Koutsoliakos^a, Edsko E.G. Hekman^b, Aakash Agarwal^c, René M. Castelein^a, Moyo C. Kruyt^a

^a Department of Orthopaedic Surgery, University Medical Center Utrecht, Utrecht, the Netherlands

^b Department of Biomechanical Engineering, University of Twente, Enschede, the Netherlands

^c Engineering Center for Orthopedic Research Excellence (E-CORE), Department of Bioengineering, University of Toledo, OH, United States

ARTICLE INFO

Keywords:

Early-onset scoliosis
Biomechanics
Distraction
Growing rods
Spine
Safety

ABSTRACT

Distraction-based growing rods are frequently used to treat Early-Onset Scoliosis. These use intermittent spinal distractions to maintain correction and allow for growth. It is unknown how much spinal distraction can be applied safely. We performed a systematic review and meta-analysis of clinical and biomechanical literature to identify such safety limits for the pediatric spine.

This systematic review and meta-analysis was performed according to the Preferred Reporting Items for Systematic Reviews and Meta-Analyses (PRISMA) statement. Three systematic searches were performed including in-vivo, ex-vivo and in-silico literature. Study quality was assessed in all studies and data including patient- or specimen characteristics, distraction magnitude and spinal failure location and ultimate force at failure were collected. Twelve studies were included, 6 in-vivo, 4 ex-vivo and 2 in-silico studies. Mean in-vivo distraction forces ranged between 242 and 621 N with maxima of 422–981 N, without structural failures when using pedicle screw constructs. In the ex-vivo studies (only cervical spines), segment C0-C2 was strongest, with decreasing strength in more distal segments. Meta-regression analysis demonstrated that ultimate force at birth is 300–350 N, which increases approximately 100 N each year until adulthood. Ex-vivo and in-silico studies showed that yielding occurs at 70–90% of ultimate force, failure starts at the junction between endplate and intervertebral disc, after which the posterior- and anterior long ligament rupture. While data on safety of distraction forces is limited, this systematic review and meta-analysis may aid in the development of guidelines on spinal distraction and may benefit the development and optimization of contemporary and future distraction-based technologies.

1. Introduction

Distraction-based growing-rods are commonly used to surgically treat Early-Onset Scoliosis (EOS), a complex 3D spinal deformity. They aim to control the curve while allowing further spinal growth. Examples are the traditional growing rod (TGR) and the magnetically controlled growing rod (MCGR) (Akbarnia et al., 2005; Cheung et al., 2012). Although widely used, the magnitude and safety margins of the forces that are exerted during these distractions is still unknown. In MCGRs, the maximum force exerted by the actuator is about 200 N, although many MCGRs transmit only a fraction after several distractions (Rushon et al., 2019). TGR distraction force is determined by the surgeon that performs the distraction surgery, and these forces are rarely measured.

Distraction forces are applied in a more controlled fashion with halo gravity traction (HGT), where forces up to 50% body weight are safely applied for several weeks (Poon et al., 2018; Yang et al., 2017; Yankey et al., 2021).

At our institution, we developed a dynamic growing-rod that exerts continuous distraction forces through a helical coil spring mounted around standard rods (Lemans et al., 2021; Wijdicks et al., 2021). During implant design, we determined that there was a paucity of knowledge on which magnitude of distraction force can be tolerated by the pediatric spine. Pragmatically, we chose a relatively low initial force of 75 N, but higher forces may be much more effective. To aid in the development and optimization of this technology and its contemporary counterparts, a basic understanding on the safety of distraction forces in the pediatric

* Corresponding author at: University Medical Center Utrecht, Department of Orthopaedic Surgery, PO Box 85500, 3508 GA, Utrecht, The Netherlands.

E-mail address: j.v.c.lemans-3@umcutrecht.nl (J.V.C. Lemans).

spine needed to be established, a topic that has not yet been addressed in previous (systematic) reviews. Therefore, we performed a systematic review and meta-analysis of the clinical and biomechanical literature to identify the best evidence for upper safety limits of distraction forces on the pediatric spine.

2. Materials and methods

This systematic review was performed according to the Preferred Reporting Items for Systematic Reviews and Meta-Analyses (PRISMA) statement (Moher et al., 2009). We systematically searched the literature for studies that investigated distraction forces on the pediatric spine or its components. The review consists of 3 separate sections: Section 1:

In-vivo studies that clinically measure distraction forces in children. Section 2: Ex-vivo biomechanical tensile tests on whole pediatric spines or spinal sections. Section 3: In-silico models that investigate load-sharing of the spine and its components in either children or adults. Since these sections are heterogeneous in study design, the search strategy was different for each section (Table 1).

2.1. Search strategy and eligibility criteria

For each section, the PubMed, Embase and Cochrane databases were systematically searched, with no restriction on publication date. We included English articles that investigated the spine or its components in distraction, and that measured or calculated distraction forces that were

Table 1
Search strategies. Date of search: 14-01-2020.

Section 1: In-vivo studies			
	PubMed	EMBASE	Cochrane
1	force[tiab]	force:ab,ti	(force):ti,ab,kw
2	distract*[tiab]	distract*:ab,ti	(distract*):ti,ab,kw
3	spine[mesh]	'spine'/exp	mesh descriptor:[spine]
4	spine[tiab]	spine:ab,ti	(spine):ti,ab,kw
5	spinal[tiab]	spinal:ab,ti	(spinal):ti,ab,kw
6	#3 OR #4 OR #5	#3 OR #4 OR #5	#3 OR #4 OR #5
7	#1 AND #2 AND #6	#1 AND #2 AND #6	#1 AND #2 AND #6
	182 results	215 results	14 results
Section 2: Ex-vivo studies			
	PubMed	EMBASE	Cochrane
1	pediat*[tiab]	pediat*:ab,ti	(pediat*):ti,ab,kw
2	paediat*[tiab]	paediat*:ab,ti	(paediat*):ti,ab,kw
3	*natal[tiab]	natal:ab,ti	(*natal):ti,ab,kw
4	child*[tiab]	child*:ab,ti	(child*):ti,ab,kw
5	adolesc*[tiab]	adolesc*:ab,ti	(adolesc*):ti,ab,kw
6	"year old"[tiab]	"year old":ab,ti	("year old"):ti,ab,kw
7	spine[ti]	spine:ti	(spine):ti
8	spinal[ti]	spinal:ti	(spinal):ti
9	vertebr*[ti]	vertebr*:ti	(vertebr*):ti
10	disc[ti]	disc:ti	(disc):ti
11	disk[ti]	disk:ti	(disk):ti
12	ligament[ti]	ligament:ti	(ligament):ti
13	physis[ti]	physis:ti	(physis):ti
14	epiphys*[ti]	epiphys*:ti	(epiphys*):ti
15	"growth plate"[ti]	"growth plate":ti	("growth plate"):ti
16	distract*[tiab]	distract*:ab,ti	(distract*):ti,ab,kw
17	tensi*[tiab]	tensi*:ab,ti	(tensi*):ti,ab,kw
18	failure[tiab]	failure:ab,ti	(failure):ti,ab,kw
19	biomech*[tiab]	biomech*:ab,ti	(biomech*):ti,ab,kw
20	force[tiab]	force:ab,ti	(force):ti,ab,kw
21	#1 OR #2 OR #3 OR #4 Or #5 OR #6	#1 OR #2 OR #3 OR #4 Or #5 OR #6	#1 OR #2 OR #3 OR #4 Or #5 OR #6
22	#7 OR #8 OR #9 OR #10 OR #11 OR #12 OR #13 OR #14 OR #15	#7 OR #8 OR #9 OR #10 OR #11 OR #12 OR #13 OR #14 OR #15	#7 OR #8 OR #9 OR #10 OR #11 OR #12 OR #13 OR #14 OR #15
23	#16 OR #17 OR #18 OR #19 OR #20	#16 OR #17 OR #18 OR #19 OR #20	#16 OR #17 OR #18 OR #19 OR #20
24	#21 AND #22 AND #23	#21 AND #22 AND #23	#21 AND #22 AND #23
	1590 Results	2083 Results	223 Results
Section 3: In-silico studies			
	PubMed	EMBASE	Cochrane
1	finite[tiab]	finite:ab,ti	(finite):ti,ab,kw
2	element[tiab]	element:ab,ti	(element):ti,ab,kw
3	"finite element analysis"[mesh]	'finite element analysis'/exp	mesh descriptor: [finite element analysis]
4	spine[mesh]	'spine'/exp	mesh descriptor: [spine]
5	spine[tiab]	spine:ab,ti	(spine):ti,ab,kw
6	spinal[tiab]	spinal:ab,ti	(spinal):ti,ab,kw
7	distract*[tiab]	distract*:ab,ti	(distract*):ti,ab,kw
8	tensi*[tiab]	tensi*:ab,ti	(tensi*):ti,ab,kw
9	failure[tiab]	failure:ab,ti	(failure):ti,ab,kw
10	#1 AND #2	#1 AND #2	#1 AND #2
11	#3 OR #10	#3 OR #10	#3 OR #10
12	#4 OR #5 OR #6	#4 OR #5 OR #6	#4 OR #5 OR #6
13	#7 OR #8 OR #9	#7 OR #8 OR #9	#7 OR #8 OR #9
14	#11 AND #12 AND #13	#11 AND #12 AND #13	#11 AND #12 AND #13
	436 results	579 results	10 results

used. Reference screening and citation tracking was performed to find additional studies. As growth-friendly implants primarily transmit a pure distraction force (and will limit flexion/extension moments), studies investigating such moments without specifying the pure distraction component were excluded. Conference abstracts, letters and (systematic) reviews were also excluded. Additional eligibility criteria per section are outlined in Table 2.

2.2. Study selection and quality assessment

Title- and abstract screening was performed by two authors (JVCL and IK). Conflicts were discussed until consensus was reached. For clinical studies, quality was assessed with the Methodological Index for Non-Randomized Studies (MINORS) instrument (Slim et al., 2003). A maximum score of 16 can be obtained for non-comparative studies, we arbitrarily defined low quality as a score below 8, moderate quality as a score between 8 and 12 and high quality as a score > 12. Since no metric to assess biomechanical- and finite element study quality was available at the time of this study, we prospectively created a quality assessment tool for each study type, based on reporting recommendations made by the US Food and Drug Administration (FDA, 2019, 2016). All three quality assessment tools and their respective criteria are outlined in Table 3.

2.3. Data extraction and statistical (meta-)analysis

Study characteristics and results regarding forces, displacement and tissue damage were extracted using standardized forms. The data of Section 2 was pooled and a meta-analysis was performed to determine relationships between age and ultimate force. Specimens were separated in three anatomical groups: C0-C2, C2-C5 and C5-T1. For each group, a least-squares second-order polynomial regression analysis was performed with age as the independent variable and ultimate force of each specimen as the dependent variable. Profile likelihood 95% confidence intervals were calculated for each regression equation and the adjusted coefficients of determination (R^2) were calculated. GraphPad Prism 8.4.1 (GraphPad Software Inc.) was used for statistical analysis.

3. Results

The literature searches of all sections yielded 5332 results. After title- and abstract screening, 64 studies remained for full-text screening. A PRISMA flowchart for each section is provided in Fig. 1.

3.1. Section 1: In-vivo studies

3.1.1. Study characteristics and -quality

Six articles were included, study characteristics and quality assessment are shown in Table 4a. Three studies investigated Harrington rod

distractions (Dunn et al., 1982; Elfstrom and Nachemson, 1973; Waugh, 1966), three reported TGR distractions (Agarwal et al., 2019; Noordeen et al., 2011; Teli et al., 2012). In one study, bilateral distraction was performed and mean force was reported (Agarwal et al., 2019), the others used unilateral distraction. Mean MINORS score was 10.8 (range 9–13) out of 16, indicating moderate to high study quality (Table 3a).

3.1.2. Force and failure results of Harrington rod distraction (Table 5a)

Waugh measured distraction force in 3 adolescent idiopathic scoliosis (AIS) patients from implantation to several hours postoperatively (Waugh, 1966). Maximum distraction force ranged from 177 to 373 N. In two patients, failures were observed; a laminar fracture at 373 N and several simultaneous transverse process (TP) fractures at 294 N. In the third patient, moments with high intra-abdominal pressure caused considerable increase of measured force (Coughing: 363 N, Vomiting: 677 N), although no failures were seen. Elfström and Nachemson used distraction force measurements in 8 AIS patients; maximum force was 422 N. There were two laminar fractures, at 235 N and 324 N (Elfstrom and Nachemson, 1973). Dunn et al. performed distraction in 12 patients in two steps; first with a slow continuous distraction outrigger, followed by the definitive, more forceful distraction (Dunn et al., 1982). Mean initial outrigger force was 332 N with a maximum of 608 N. During the forceful distractions, mean and maximum force increased to 627 N and 981 N respectively. During distraction, a laminar fracture in a patient with osteopenic bone occurred at 392 N. In all three studies, stress-relaxation was observed starting with a 40% reduction in residual forces during 30–60 min post-operatively. One study measured post-operative forces continuously for 2 weeks (Elfstrom and Nachemson, 1973). A further reduction in distraction forces took place so that only 40% of the force remained after 4 days. After 11 days, the unilateral residual force was relatively stable at 25% of the initial force, corresponding to around 100 N.

3.1.3. Force and failure results of TGR distraction (Table 5a, Fig. 2)

Teli et al. investigated how forces increase during every subsequent millimeter of distraction during the first distraction episode (Teli et al., 2012). After a threshold force of 133 N, there was a linear increase in force up to the 12th millimeter of distraction. The two other studies investigated overall increase in applied force with subsequent distractions (Agarwal et al., 2019; Noordeen et al., 2011). Mean distraction force increased from 140 to 142 N during the first distraction to 515–555 N for the latest. Maximally applied forces ranged between 552–645 N. One TGR study reported a failure, a laminar fracture at around 450 N (Agarwal et al., 2019).

3.2. Section 2: Ex-vivo studies

3.2.1. Study characteristics and -quality

Four articles were included, study characteristics and quality

Table 2
Eligibility criteria.

	Inclusion criteria	Exclusion criteria
Section 1: In-vivo studies	<ul style="list-style-type: none"> - In-vivo study - Age < 18 years - Investigates spinal distraction 	<ul style="list-style-type: none"> - No quantitative force/stress data - No English language - Case reports, letters, reviews
Section 2: Ex-vivo studies	<ul style="list-style-type: none"> - Biomechanical ex-vivo study of spine or spinal component - Age < 18 years - Investigates pure tension/distraction 	<ul style="list-style-type: none"> - Animal studies - Only reports data on implants - No quantitative force/stress data - No English language - Case reports, letters, reviews
Section 3: In-silico studies	<ul style="list-style-type: none"> - In-silico study - Investigates the spine with at least 1 functional spinal unit - Investigates pure tension/distraction 	<ul style="list-style-type: none"> - Animal studies - Only reports data on implants - No quantitative force/stress data - Only gives results of single spinal component - No English language - Case reports, letters, reviews

Table 3
Study quality assessment.

(a) MINORS study quality for in-vivo studies											
Author(s)	Aim	Consecutive patients	Prospective data collection	Appropriate endpoints	Unbiased assessment	Appropriate follow-up	Loss to follow-up < 5%	Prospective study size calculation			Total
Wagh	2	0	1	1	1	2	2	0			9/16
Elfström and Nachemson	2	0	1	2	1	2	2	0			10/16
Dunn et al.	2	0	1	1	2	2	2	0			10/16
Noordeen et al.	2	2	2	2	1	2	2	0			13/16
Teli et al.	2	0	1	2	1	2	2	0			10/16
Agarwal et al.	2	2	2	2	1	2	2	0			13/16
Low Quality: 0–7; Moderate Quality: 8–12; High Quality: 13–16											
(b) Study quality for ex-vivo studies											
Author(s)	Aim	Protocol	Sample size	Specimens	Harvesting and treatment	Testing machine	Preconditioning and loading	Specimen accountability	Reporting force	Reporting failure	Total
Duncan	2	0	0	1	0	1	1	2	2	0	9/20
Ouyang et al.	2	2	1	2	2	2	2	1	2	1	17/20
Luck et al.	2	1	0	2	2	2	2	2	2	2	17/20
Nuckley et al.	2	1	0	2	2	2	2	2	2	1	16/20
2 points: Adequately reported. Enough information to replicate experiment. 1 point: Reported but inadequate/unclear. Insufficient detail to replicate experiment. 0 points: Not reported. Low Quality: 0–10; Moderate Quality: 11–15; High Quality: 16–20 Aim: The research question of the investigation is explained, and this question can be answered through the proposed research. Protocol: A test protocol was prospectively created and all samples adhered to this protocol. Sample size: The number of included specimens was prospectively calculated and allows for valid comparisons between investigated groups. Specimens: A representative subset of the population is chosen to provide the specimens. Specimen characteristics (age, sex, weight) are reported. Harvesting and treatment: The condition under which the specimens were harvested, stored and prepared for the experiment are explained in detail and are identical for all specimens. Testing machine: The characteristics of the testing machine are reported, and the experimental set-up is explained in detail or is shown in a figure. Preconditioning and loading: Preconditioning steps and loading rate are reported. Specimen accountability: Data is reported for all specimens, including outliers/anomalous results. For specimens with failed measurements, a detailed explanation is provided. Reporting force: Force results are reported for individual specimens. Reporting failure: Failure results are reported and detailed reporting is provided for each specimen explaining which structure(s) (if any) failed.											
(c) Study quality for in-silico studies											
Author(s)	Aim	Solver	Geometry and mesh	Material Properties	Assumptions and simplifications	Boundary- and loading conditions	Results	Mesh refinement	Validation	Total	
DeWit and Cronin	2	2	2	2	1	2	2	2	1	16/18	
Dong et al.	2	2	2	1	2	2	2	2	2	17/18	
2 points: Adequately reported. Enough information to replicate experiment. 1 point: Reported but inadequate/unclear. Insufficient detail to replicate experiment. 0 points: Not reported. Low Quality: 0–8; Moderate Quality: 9–13; High Quality: 14–18 Aim: The research question of the investigation is explained, and this question can be answered through the proposed research. Solver: The software package, version and type of simulation are reported. Geometry and mesh: The finite element geometry is presented in detail. This includes an explanation on how the geometry was obtained and includes details on elements and mesh used. Material properties: Material properties for all materials are included and referenced. Assumptions and simplifications: Differences with and simplifications of the model to the real-world situation are described (e.g. a rationale is provided for structures not included in the model). Boundary and loading conditions: Boundary conditions are explained. Initial conditions, pre-stresses and loading conditions are provided. Results: A relevant outcome measure was chosen and results were provided for several relevant regions in the finite element model. Mesh refinement: A mesh was chosen so that outcomes were not significantly influenced by element size. This was tested with mesh refinement or convergence analysis techniques. Validation: Results were validated to existing clinical or biomechanical data and were in accordance to that data.											

assessment are shown in Table 4b. All investigated tension to failure in pediatric cervical spines. One study exclusively investigated neonatal spines (Duncan, 1874), the others investigated a range of age groups, from neonates to adolescents (Luck et al., 2013; Nuckley et al., 2013; Ouyang et al., 2005). No studies investigated individual pediatric spinal components like the intervertebral disc (IVD), epiphyseal plate or spinal ligaments. Mean quality score was 14.8 (range 9–17) out of 20 (Table 3b). One study had low study quality (Duncan, 1874), while the other three had high study quality.

3.2.2. Force and failure results (Table 5b, Fig. 3)

Already in 1874, Duncan investigated the force needed to sever the cervical spine in stillborn infants (Duncan, 1874). Increasing force was applied by weights through a pulley system. Mean force needed was 507 ± 95 N. All spines failed between C3 and C7, the structure that failed first was not reported. The other three studies tested ultimate force

($F_{ultimate}$) at different ages in displacement controlled experiments. Ultimate force was defined as the highest force recorded followed by a sudden decrease in reaction force with continued displacement and coincident with gross evidence of tissue damage (i.e. failure of the strongest spinal component). Luck et al. investigated the $F_{ultimate}$ of three different cervical levels in children of three different age groups (<2 years old, 6–9 years, 12–17 years) (Luck et al., 2013). In all age groups, C0-C2 showed the highest $F_{ultimate}$. In all levels, $F_{ultimate}$ increased non-linearly with age, with a 3–4-fold increase during the first 6–9 years and a 1.5–2.5-fold increase between 6 and 9 years and adulthood. For C0-C2, $F_{ultimate}$ increased from a mean of 436 ± 363 N in children < 2 to 2714 ± 230 N in adolescents. For C4-C5, $F_{ultimate}$ increased from 317 ± 198 N to 2030 ± 302 N. For C6-C7, these values were 292 ± 186 N and 1832 ± 259 N.

When correcting for vertebral cross-sectional area, ultimate tensile strength (UTS) also increased with age, albeit less sharply. For C6-C7,

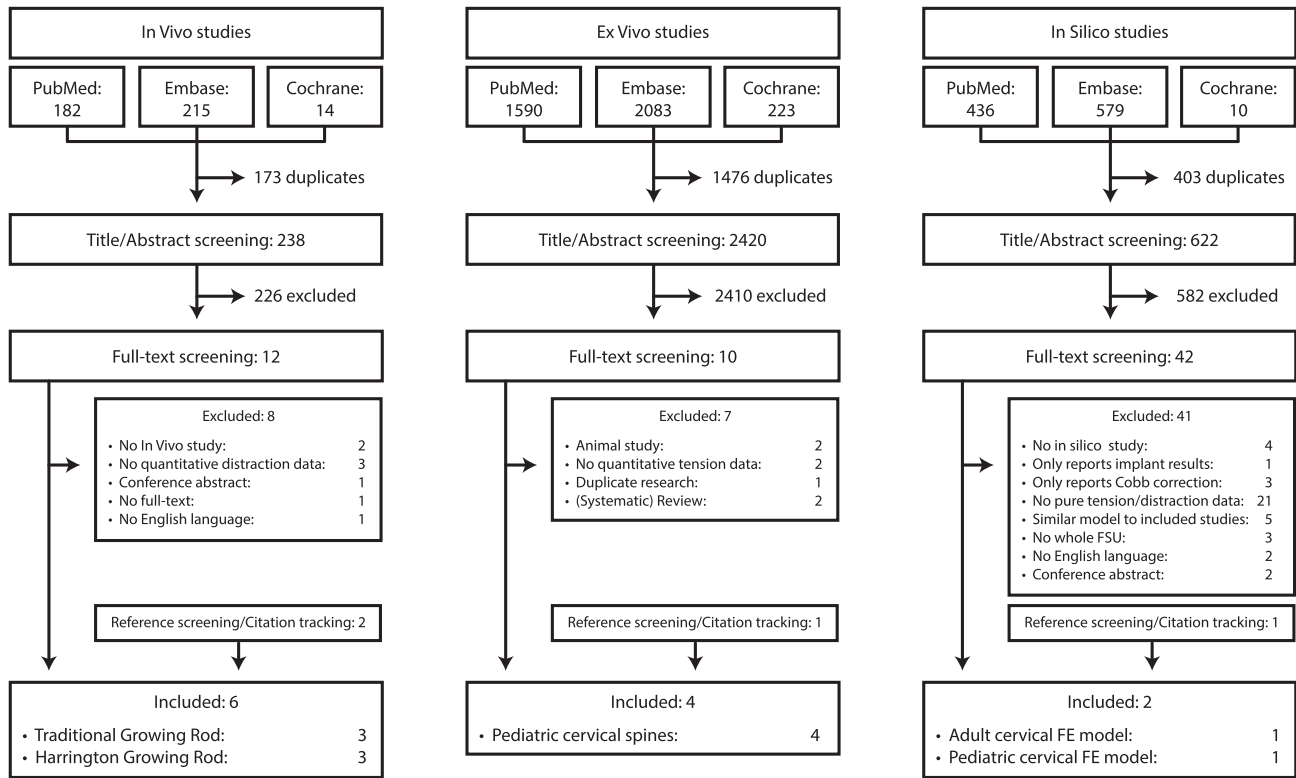


Fig. 1. PRISMA diagram.

UTS was 2.7 ± 0.6 MPa for children < 2 years and 5.3 ± 1.2 MPa for adolescents. In the spines < 2 years old, failure occurred almost exclusively through the epiphyseal plate or through the cartilaginous synchondrosis. The two older age groups failed through the epiphyseal plate in half of the cases, in the other half, failure occurred at either the vertebral body or the IVD. Luck et al. also investigated yield force (F_{yield}), defined as the first point of lower force increase with continued displacement and coincident with visual spinal damage (i.e. failure of the weakest spinal component). Overall, F_{yield} was only slightly ($\sim 10\%$) lower than $F_{ultimate}$; C0-C2 showed an F_{yield} of 1016 ± 909 N versus $F_{ultimate}$ of 1116 ± 993 N. For C4-C5, these values were 652 ± 608 N and 705 ± 649 N respectively, and for C6-C7, they were 618 ± 576 N (3.0 MPa) and 694 ± 634 N (3.4 MPa). Ouyang et al. investigated $F_{ultimate}$ in entire cervical spines (C0-T1) in two age groups, 2–4 year olds and 6–12 year olds (Ouyang et al., 2005). In the younger group, mean $F_{ultimate}$ was 609 ± 114 N. In older children, $F_{ultimate}$ was 872 ± 62 N. All failures occurred in the distal cervical spine, the exact structures that failed were not reported. Nuckley investigated $F_{ultimate}$ in level C1-C2 in two age groups, 2–8 year old children and 9–16 year old children (Nuckley et al., 2013). In the younger group, mean $F_{ultimate}$ was 983 ± 265 N. For the older children this was 1669 ± 109 N. All failures were ligamentous failures.

Meta-analysis of the ex-vivo studies is shown in Fig. 3. Residuals were normally distributed. Adjusted R^2 values of the cubic functions of different segments ranged between 0.82 and 0.86, indicating that most variation could be explained by age alone. In all segments, an increase in $F_{ultimate}$ was seen with increasing age. For C0-C2, this increase was largest during the first years, for the other segments, the increase followed a more linear trend. For the distal segments, increase in $F_{ultimate}$ was approximately 100 N/year. From infancy to end of adolescence, $F_{ultimate}$ increased from 341 N to 2453 N in C0-C2, from 342 N to 2190 N in C2-C5 and from 294 N to 1902 N in C5-T1.

3.3. Section 3: In-silico studies

3.3.1. Study characteristics and -quality

Two articles were included, study characteristics and quality assessment are shown in Table 4c. Dong et al. investigated tension to failure in an osseoligamentous FE model of a 10-year old cervical spine (Head-T1) (Dong et al., 2013), whereas DeWit and Cronin explored tensile failure in a single adult osseoligamentous functional spinal unit (C4-C5) (DeWit and Cronin, 2012). Both studies used models that included vertebral bodies, IVDs and (non-linear) ligaments. Dong et al. also included the epiphyseal plate. Both studies modelled failure, deleting elements of specific spinal components as they were loaded above their failure limit. This ensured a gradual reduction of the load-carrying capacity of the spine and permitted a detailed characterization of when and where failure occurred. Due to modelling constraints, DeWit and Cronin modelled the connection between cartilaginous endplate and IVD with tie-break elements, potentially reducing bio-fidelity of their failure modelling. Both studies validated their model to the respective adult or pediatric experimental literature. Mean study quality was 16.5 (range 16–17) out of 18, indicating high study quality (Table 3c).

3.3.2. Distraction force, load sharing and failure results

The adult C4-C5 FE segment from DeWit and Cronin was validated against previous experimental tensile data (Dibb et al., 2009). During increasing displacement, several distinct peaks were seen where failure occurred (Fig. 4). The first failure was a rupture between the posterior junction of the vertebral endplate and IVD at around 2600 N. With increasing IVD-endplate avulsion, the posterior long ligament (PLL; ~ 2500 N), anterior long ligament (ALL; ~ 2500 N) and anterior IVD-endplate junction failed (~ 1750 N). Dong et al. created an FE model that was validated against previous tensile pediatric cadaver experiments (Luck et al., 2013; Ouyang et al., 2005). When simulating tension to failure at C4-C5, first failure occurred at the IVD-endplate junction at around 650 N. This is lower than the $F_{ultimate}$ or F_{yield} reported by Luck et al. However, at this point, only a small decrease in force was observed,

Table 4
Study characteristics.

(a) In-vivo studies									
Author(s)	Year	Number of patients ^a	Patient type (N)	Mean age	Investigated spine location	Type of distraction	Proximal-distal anchors	MINORS score	
Waugh	1966	3	AIS (3)	14.7±0.5 yr	Thoracic-Lumbar	Harrington rod (unilateral)	1 Hook-1 Hook	9/16 (Moderate)	
Elfström and Nachemson	1973	8	AIS (8)	14.0±1.6 yr	Thoracic-Lumbar	Harrington rod (unilateral)	1 Hook-1 Hook	10/16 (Moderate)	
Dunn et al.	1982	12	AIS (9), EOS (S:3)	14.7±4.3 yr	Thoracic-Lumbar	Harrington rod (unilateral)	1 Hook-1 Hook	10/16 (Moderate)	
Noordeen et al.	2011	26	EOS (I:4, S:3, NM:9, C:9)	6.5±2.3 yr	Thoracic-Lumbar	TGR (unilateral)	3 Hooks-2 Screws	13/16 (High)	
Teli et al.	2012	10	EOS (I:4, S:3, C:1, U:2)	8.3 (6–10) yr	Thoracic-Lumbar	TGR (unilateral)	2 Hooks-1 Screw + 1 Hook	10/16 (Moderate)	
Agarwal et al.	2019	47	EOS (I:4, S:1, NM:2, C:40)	7.2±2.3 yr	Thoracic-Lumbar	TGR (bilateral)	2 Hooks-2 Screws ^b	13/16 (High)	

MINORS: Methodological Index for Non-Randomized Studies; AIS: Adolescent Idiopathic Scoliosis; EOS: Early Onset Scoliosis; TGR: Traditional Growing Rod; TP: Transverse Process; I: Idiopathic; S: Syndromic; NM: Neuromuscular; C: Congenital; U: Unknown.
^aOnly patients under age 18 were included.
^bUsed bilaterally.

(b) Ex-vivo studies										
Author(s)	Year	Number of cadavers (specimens)	Specimen age (N) ^a	Investigated spine location (N)	Preparation of spine	Study method	Distraction system	Testing method and rate	Endpoint	Study quality
Duncan	1874	5 (5)	≤1 day (4) 0 yr (1)	C0-C7 (5)	Intact	Head fixed with rods at shoulders, weights added to ankles.	Manual adding of weight to pulley	Force controlled: Steps of several lbs every 30 s.	Complete severing of the cervical spine	9/20 (Low)
Ouyang et al.	2005	9 (9)	2 yr (2) 3 yr (2) 4 yr (1) 6 yr (2) 7 yr (1) 12 yr (1)	C0-T1 (9)	Removal of muscles, subcutaneous tissues.	Cranium and caudal vertebra potted and fixed to actuator in experimental frame. Then, non-destructive tests in flexion/extension and viscoelastic characterization. Then, tension until failure.	Mini-Bionix 858 MTS (MTS Systems Corp., Eden Prairie, MN, USA)	Displacement controlled: 5 mm/s.	Failure: 10% decrease in tensile load with increasing displacement.	17/20 (High)
Luck et al.	2013	23 (58) ^b	≤1 day (14) 0 yr (20) 1 yr (5) 6 yr (3) 7 yr (3) 9 yr (3) 12 yr (3) 14 yr (1) 16 yr (3) 17 yr (3)	C0-C2 (18) C4-C5 (21) C6-C7 (19)	Removal of muscles and subcutaneous tissues.	Cranial vertebra/cranium and caudal vertebra potted and fixed to actuator in experimental frame. Then, tension until failure.	MTS (MTS Systems Corp., Eden Prairie, MN, USA)	Force controlled: 1000 N/s * scale factor based on T1 endplate size ^c Displacement controlled: 230 mm/s ^d	Failure: Load decrease with increasing displacement. Ultimate force: Maximum force in force–displacement curve.	17/20 (High)
Nuckley et al.	2013	8 (8)	2 yr (1) 3 yr (1) 5 yr (1) 8 yr (1) 9 yr (1) 11 yr (1) 13 yr (1) 16 yr (1)	C1-C2 (8)	Removal of muscles and subcutaneous tissues.	Cranial and caudal vertebrae potted, then non-destructive tests in compression, tension and bending. Then tension until failure.	MTS 318.10S (MTS Systems Corp., Eden Prairie, MN, USA)	Displacement controlled: 1000 mm/s.		16/20 (High)

NR: Not reported
^aSpecified per year, 0–1 day old neonates reported separately.
^bSeveral specimens included pre-term infants (>20 weeks gestation). These were counted as age ≤ 1 day.
^cFor specimens aged 0 days-5 months and 14 year old.
^dFor specimens aged > 5 months-9 years.

(continued on next page)

Table 4 (continued)

(c) In-silico studies									
Author(s)	Year	FEA program	Model	Included component	Material properties	Yield properties	Failure modelling	Tensile validation	Study quality
DeWit and Cronin	2012	LS-DYNA v.971 (LSTC, Livermore, CA,USA)	Male, adult C4-C5	Cortical bone	E = 17,900 $\nu = 0.3$	$\sigma = 190$ $\epsilon = 1.8$	Gradually removing elements as the critical failure stress was reached. Tie-break contacts were chosen for the disc-vertebra interface. These were broken as the failure stress was reached.	C4-C5 (Dibb et al., 2009)	16/18 (High)
				Cancellous bone	E = 55.6 $\nu = 0.3$	$\sigma = 4.0$ $\epsilon = 6.7$			
				Bony endplate	E = 5967 $\nu = 0.3$	$\sigma = 63.3$ $\epsilon = 1.8$			
				Cartilaginous endplate	E = 23.8 $\nu = 0.4$	$\sigma = 53.3^b$			
				Annulus fibrosis	Shell elements in ground substance				
				Nucleus pulposus	K = 1720				
				ALL, PLL, LF, CL, ISL	Sigmoidal curves based on literature. (Chazal et al., 1985, Yoganandan et al., 2001)				
Dong et al.	2013	LS-DYNA v.971 (LSTC, Livermore, CA,USA)	Male, 9 years Head-T1	Cortical bone ^a	E = 13,400 $\nu = 0.3$	NS	Gradually removing elements as the critical failure stress was reached.	C4-C5 (Luck et al., 2013) C6-C7 (Luck et al., 2013) Head-T1 (Ouyang et al., 2005)	17/18 (High)
				Cancellous bone ^a	E = 241 $\nu = 0.3$				
				Bony endplate ^a	E = 4480 $\nu = 0.3$				
				Cartilaginous endplate ^a	E = 23.8 $\nu = 0.4$	$\sigma = 30$			
				Epiphyseal plate	E = 25 $\nu = 0.4$				
				Annulus fibrosis ^a	Shell elements in ground substance				
				Nucleus pulposus	K = 1720				
				ALL, PLL, LF, CL, ISL ^a	Sigmoidal curves based on literature. (Chazal et al., 1985, Yoganandan et al., 2000, 2001)				

NA: Not applicable; NS: Not simulated
E: Young's modulus (MPa); ν : Poisson's ratio; σ : Stress (MPa); ϵ : Strain (%); K: Bulk modulus
^aReported values were the used adult values, these were scaled down to pediatric values.
^bCorresponding to a stress of 4.70 MPa across the entire disc and cartilaginous endplate.

Table 5
Results of forces used and evidence of spinal failure.

(a) In-vivo studies							
Author(s)	Year	Mean force	Maximum force ^a	Force at failure	Structural damage		
Waugh	1966	242 ± 46 N	677 N	373 N 294 N	Proximal laminar fracture Multiple simultaneous transverse process #		
Elfström and Nachemson	1973	288 ± 89 N	422 N	235 N 324 N	Proximal laminar fracture Proximal laminar fracture		
Dunn et al.	1982	621 ± 251 N	981 N	392 N	Proximal laminar fracture		
Noordeen et al.	2011	335 ± 170N ^b	645 N	NR	NR		
Teli et al.	2012	331 ± 96 N	552 N	No failure	No failure		
Agarwal et al.	2019	311 ± 114N ^b	578 N	455N ^c	Proximal laminar fracture		

NR: Not reported; #: fracture
^aMaximum force recorded during or after distraction.
^bMean force across all distraction episodes.
^cNo data for exact case, mean force at distraction episode during which damage occurred was taken.

(b) Ex-vivo studies							
Author(s)	Year	Number of specimens	Segment tested (N)	Age group (N) ^a	Failure level (N)	Ultimate force ^b	Structural damage (N)
Duncan	1874	5	C0-C7 (5)	≤1 day (4)	C4-C5 (2) C5-C6 (1) C6-C7 (1)	405N-543N 400N 534N	NR (2) NR (1) NR (1)
				1 day-2 years (1)	C3-C4 (1)	654N	NR (1)
Ouyang et al.	2005	9	C0-T1 (9)	2-5 years (5)	C5-C6 (2) C6-C7 (1) C7-T1 (2)	494N-817N 570N 531N-634N	# superior endplate C6 (2) # inferior endplate C7 (1) # superior endplate T1 (1); # inferior endplate C7 (1)
				5-10 years (3)	C4-C5 (1) C6-C7 (1) C7-T1 (1)	892N 912N 765N	# superior endplate C5 (1) # superior endplate C7 (1) # superior endplate T1 (1)
				>10 years (1)	C7-T1	918N	# inferior endplate C7 (1)
Luck et al.	2013	58 ^b	C0-C2 (18)	≤1 day (4)	C1-C2 (2) C2-C3 (2)	197N-275N 209N-242N	Atlanto-axial dislocation with Type III dens # (2) C2-C3 dislocation + multiple C2 # (1); Epiphyseal # inferior endplate C2 + multiple C3 # (1)
				1 day-2 years (7)	C1-C2 (3) C2-C3 (4)	462N-1231N 174N-840N	Atlanto-axial dislocation with Type III dens # (2); Atlanto-axial dislocation + ossiculum terminale # of dens (1) C2-C3 dislocation + multiple C2 # (2); Epiphyseal # inferior endplate C2 (1); C2-C3 dislocation + type III dens # (1)
				5-10 years (3)	C0-C1 (1) C1-C2 (1) C2-C3 (1)	1761N 1927N 1425N	Basilar skull # + occipito-atlantal facet capsule disruption (1) Atlanto-axial dislocation + ossiculum terminale # of dens (1) C2 inferior vertebral body # + type III dens # (1)
				>10 years (4)	C0-C1 (3) C2-C3 (1)	2703N-2970N 2350N	Occipito-atlantal + partial atlanto-axial dislocation + medial # of left condyle + avulsion of right alar ligament (1); Occipito-atlantal dislocation + C1 # in right anterior arch + right occipital condyle # (1); Occipito-atlantal dislocation (1) C2 inferior vertebral body # + bilateral spinous process (1)
			C4-C5 (21)	≤1 day (6)	C4-C5 (4) C5-C6 (2) C3-C4 (3)	174N-360N 57N-181N 183N-631N	Epiphyseal # superior endplate C5 (2); Epiphyseal # inferior endplate C4 + right neurocentral synchondrosis to posterior synchondrosis # C4 (1); Epiphyseal # inferior endplate C4 (1) Epiphyseal # inferior endplate C5 (1); Epiphyseal # superior endplate C6 (1) Epiphyseal # superior endplate C4 + bilateral C4 neurocentral synchondroses # + bilateral C5 lamina # (1); Epiphyseal # superior endplate C4 (2)
				1 day-2 years (9)	C4-C5 (5) C5-C6 (1)	167N-916N 330N	Epiphyseal # inferior endplate C4 (4); Epiphyseal # superior endplate C5 (1) Epiphyseal # inferior endplate C5 (1)
				5-10 years (3)	C4-C5 (3)	700N-1214N	Epiphyseal # superior endplate C5 + C4 body fracture (1); Complete ligamentous and IVD disruption (1); Epiphyseal # superior endplate C5 (1)
				>10 years (3)	C4-C5 (3)	1732N-2444N	Complete ligamentous and intervertebral disc disruption + epiphyseal # inferior endplate C4 (1); C5 lamina and spinous process # + C4 vertebral body # and disruption endplate/IVD + complete ligamentous disruption (1); Epiphyseal # inferior endplate C4 (1)
			C6-C7 (19)	≤1 day (4)	C6-C7 (3) C7-T1 (1)	154N-210N 181N	Epiphyseal # superior endplate C7 (3) Epiphyseal # inferior endplate C7 (1)

(continued on next page)

Table 5 (continued)

Nuckley et al.	2013	8	C1-C2 (8)	1 day-2 years (9)	735N	Epiphyseal # superior endplate C5 (1)
				5-10 years (3)	142N-800N	Epiphyseal # superior endplate C6 + unilateral right C6 neurocentral synchondrosis # (1); Epiphyseal # superior endplate C6 (3)
				>10 years (3)	152N-417N	Epiphyseal # inferior endplate C6 (1); Epiphyseal # superior endplate C7 (3)
				2-5 years (2)	864N	C6 vertebral body fracture (1)
				5-10 years (3)	814N-1758N	Complete ligamentous and IVD disruption (1); Epiphyseal # inferior endplate C6 (1)
				>10 years (3)	1570N-	Complete ligamentous and IVD disruption + Epiphyseal # inferior endplate C6 (1); C6 lamina and spinous process # + C7 vertebral body # + C7 lamina and spinous process # (1); Epiphyseal # inferior endplate C6 (1)
				2-5 years (2)	2185N	Unspecified ligamentous failure (1) + type II dens # (1)
				5-10 years (3)	582-1102	Unspecified ligamentous failure (3)
				>10 years (3)	941-1543	Unspecified ligamentous failure (3)
				>10 years (3)	1588-1817	Unspecified ligamentous failure (3)

^aFive groups were created: (1) ≤1 day, (2) 1 day-2 years, (3) 2-5 years, (4) 5-10 years, (5) >10 years.

^bSeveral specimens included pre-term infants (> 20 weeks gestation). These were counted as age ≤ 1 day. NR: Not reported, #: fracture, IVD: Intervertebral disc.

indicating minor failure. With increasing distraction, larger decreases in force are seen indicating failure of the PLL (~890 N), followed by failure of the ALL together with the IVD-endplate junction (1060 N). For C6-C7, first failure occurred at the IVD-endplate junction (~1330 N) and F_{ultimate} occurred with a PLL rupture (~1620 N). When simulating a whole cervical spine (Head-T1), first failure occurred at much higher displacement (as expected) and at a force of around 1025 N at the inferior IVD-endplate junction of C2.

4. Discussion

Although distraction of the spine is often applied in deformity correction, we know little about its safety limits. Forces are generally applied based on previous experiences and common knowledge. The current study was an effort to get a better understanding of what forces can be applied safely for novel distractive implants.

In general, there was a paucity of literature on the pediatric thoracic spine where distraction implants are usually implanted. Relevant literature indicates that the force that can be applied to the pediatric spine is several times the force of body weight, much higher than forces used in HGT, TGR or MCGR. If spinal integrity fails, this is usually at or around the endplate. The resistance to failure of this structure increases with the increase in cross-sectional area during growth, but also independent of this, due to maturation (Luck et al., 2013). As the maturation effect has also been observed quite similarly in animal species, this could enable future in-vivo research on distraction safety and efficacy (Ching et al., 2001; Pintar and Mayer, 2000).

Since most studies investigated forces during only short periods of time, important phenomena like creep and stress relaxation were ignored. Creep properties of spinal components in tension have not been studied extensively, although its effect must take place as shown by HGTs effectiveness over time (Yang et al., 2017; Yankey et al., 2021). The included Harrington rod studies show that stress relaxation most certainly takes place during distraction surgery, where distraction forces decreased 60-75% during the first post-operative weeks. However, as distraction forces decrease non-linearly, even a micro-slippage in the Harrington rod itself could have resulted in substantial reduction of residual forces.

The FEM studies suggest that the epiphyseal plate fails first, followed by the PLL and subsequently the ALL. This pattern seems to be in accordance with those reported in the ex-vivo literature, although F_{ultimate} in the FEM studies is lower (Luck et al., 2013). It could be that micro-failures (apparent only through changes in the force-displacement diagram) are missed in the in-vivo and ex-vivo studies as they are not coincident with obvious visual changes. Potentially, such micro-failures of spinal tissues play an important role in autofusion of the spine and the "law of diminishing returns" (Cahill et al., 2010; Williams et al., 1999). As micro-failures are hard to quantify in-vivo and were not subject of the current study, a safety margin should be adopted when choosing a maximum force that is to be applied. In addition, the results of the FEM studies must be interpreted with caution as many different pediatric spinal material and interaction properties are still unknown and had to be estimated from adult values (DeWit and Cronin, 2012; Dong et al., 2013; Jebaseelan et al., 2012; Kumaresan et al., 2000). Uncertainty margins of these estimations may cause large deviations in outcomes, as shown previously (Dreischarf et al., 2014; Naserkhaki et al., 2018).

Unfortunately, while an extensive search was performed, most studies that were identified focused exclusively on the cervical spine, while distraction-based therapy for EOS is primarily performed in the thoracic- and lumbar spine. Therefore, a definitive answer to our research question cannot be given. Nevertheless, due to the increase in cross-sectional area of vertebral structures from cranial to caudal, these are likely stronger than cervical segments (Myklebust et al., 1988; Yoganandan et al., 1996, 1988). The observation that HGT complications almost exclusively occur in the cervical spine also suggests that the

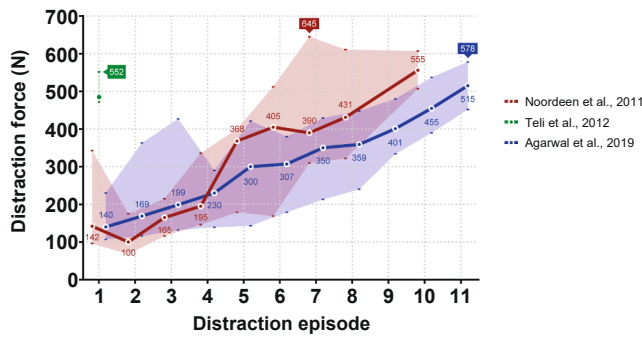


Fig. 2. Distraction force and failures in traditional growing rod studies. Mean (Agarwal et al., 2019; Teli et al., 2012) or median (Noordeen et al., 2011) forces with ranges are provided for each distraction episode.

cervical structures are weakest and that the current results are therefore likely lower bounds of the true maximum, safe distraction force (Yang et al., 2017; Yankey et al., 2021). In addition, most included ex-vivo studies investigated the spine with all muscles and subcutaneous tissues removed, which has been shown to further reduce spinal strength by a factor of 2 (Duncan, 1874; Yoganandan et al., 1996). Taking this into account, we can make several inferences for clinical practice based on current literature. While speculative, they represent the best available evidence:

1. In-vivo literature shows that distractions of 300–400 N are common, without risk of macro-failure (when not using laminar or TP hooks).
2. Ex-vivo literature shows that $F_{ultimate}$ of spinal segments increases with age in a more or less linear fashion. This $F_{ultimate}$ is 300 N at birth, and increases around 100 N each year.
3. In-silico literature shows that first failure occurs at around 70–90% of $F_{ultimate}$ at the level of the endplate, followed by failure of the PLL and ALL.
4. Adjusting for these factors, the conservative $F_{ultimate}$ of the pediatric spine becomes approximately 800 N (age 5–6), 1000 N (age 7–8) and 1200 N (age ≥ 9).

Obviously, a margin of safety must be applied to account for individual variability and the fact that there is a paucity of data on several spinal regions. A reasonable safety factor of 4 will result in a potential maximum force of 200 N (age 5–6), 250 N (age 7–8) and 300 N (age ≥ 9) when using pedicle screw anchors. Anatomical structures at risk and bone- or soft-tissue weakness may require lowering distraction forces further. Special care must be taken to avoid excessive stress on the spinal cord and nerve roots, which have been associated with certain correction manoeuvres (Henao et al., 2018). Whether these stresses are generated following axial distraction in growing-rod surgery is unknown, although neurological complications during spinal distraction are rarely seen (Agarwal et al., 2019; Noordeen et al., 2011; Teli et al., 2012; Yang et al., 2017).

The current study gives an approximation to the upper limit of corrective forces that can be applied to the pediatric spine. Whether maximum forces are also most effective has yet to be studied. There is

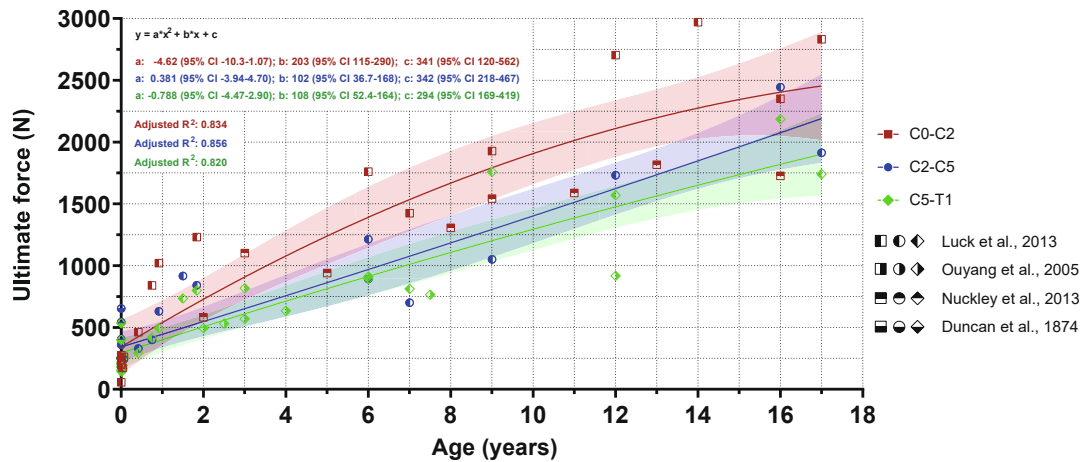


Fig. 3. Relation between age and ultimate force of the cervical spine. Meta-regression analysis was performed of all ex-vivo studies. For three cervical segments, the effect of age on ultimate force with adjusted R^2 values are shown as well as polynomial regression curves (with 95% confidence intervals).

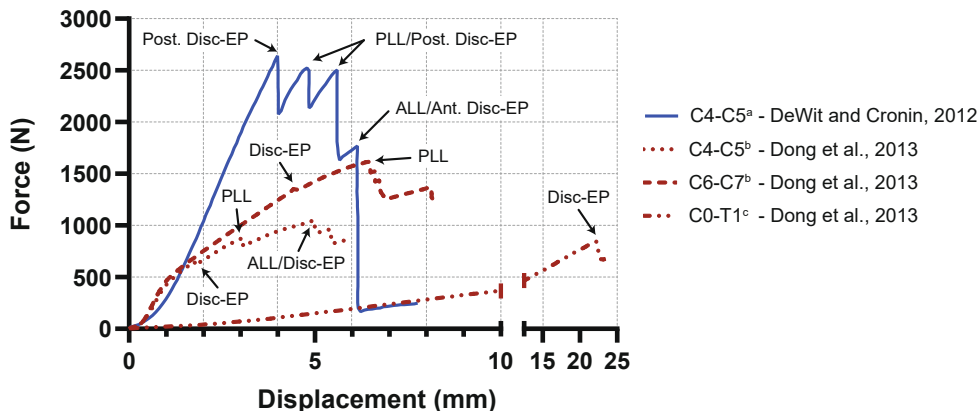


Fig. 4. Tension to failure results in the finite element method simulations. In the finite element studies, the simulated vertebrae were distracted until sequential failures occurred. The exact location of failure and the force and displacement at failure were calculated for several spinal levels. EP: Endplate (including epiphyseal plate in the pediatric model); ALL: Anterior long ligament; PLL: Posterior long ligament ^aMaterial properties: (Dibb et al., 2009), ^bMaterial properties: (Luck et al., 2013), ^cMaterial properties: (Ouyang et al., 2005).

evidence that frequent distractions with lower force improves curve correction, mitigates the “law of diminishing returns” and reduces complication rate (Agarwal et al., 2018, 2017; Cheung et al., 2016). Elucidation of these force-effects on different spinal components and implants could lead to optimization of both novel and contemporary growing-rod techniques.

This is an attempt to review safety limits of spinal distraction forces across several clinical and biomechanical domains. This approach allows for the synthesis of data from seemingly isolated research modalities which is useful in many fundamental and clinical sciences. Limitations include the low number of studies that could be included, and the fact that the ex-vivo and in-silico studies investigated only the cervical spine and not the thoracic and lumbar spine, which are most often instrumented. While this makes it difficult to draw definitive conclusions, the included studies are currently the best available evidence, which underscores the need for continued research on this important topic of spinal distraction.

5. Conclusion

Literature on safe distraction forces for the pediatric spine is limited. Clinically applied distraction forces of 300–500 N were frequently applied. Occasionally, this resulted in laminar- or TP fractures, but no study reported ligamentous disruptions or epiphyseal plate fractures. Ex-vivo cervical studies show that F_{ultimate} is around 300 N at birth and increases 100 N each year, a 6–7 fold increase from birth to end of adolescence. In-silico studies show that yielding starts at 70–90% of F_{ultimate} and that the junction between IVD and vertebral endplate fails first.

Declaration of Competing Interest

A. Agarwal is consultant for Spinal Balance Inc., member of the editorial board for Clinical Spine Surgery (LWW), Spine (LWW) and member of the advisory board for the Center for Disruptive Musculoskeletal Innovation. R.M. Castelein and M.C. Kruyt have received a Stryker Spine Research Grant unrelated to the current research. R.M. Castelein and M.C. Kruyt are the inventors of the Spring Distraction System (patent owned by UMC Utrecht Holding B.V.). R.M. Castelein and M.C. Kruyt are exploring the option of establishing a start-up company relating to this patent. The other authors declare that they have no conflict of interest.

Acknowledgements

None.

Funding statement

The authors and/or their institutions did not receive financial support for this study.

Ethics review statement

No ethical review was deemed necessary for this systematic review and meta-analysis.

Exclusivity statement

The manuscript and/or its contents have not been published elsewhere and are currently not under consideration by another journal.

Authorship statement

All authors declare that they:

1) Made substantial contributions to the conception or design of the

work; or the acquisition, analysis, or interpretation of data; or the creation of new software used in the work;

2) Drafted the work or revised it critically for important intellectual content;

3) Approved the version to be published; and..

4) Agree to be accountable for all aspects of the work in ensuring that questions related to the accuracy or integrity of any part of the work are appropriately investigated and resolved.

References

- Agarwal, A., Agarwal, A.K., Jayaswal, A., Goel, V.K., 2017. Outcomes of Optimal Distraction Forces and Frequencies in Growth Rod Surgery for Different Types of Scoliotic Curves: An In Silico and In vitro Study. *Spine Deform.* 5, 18–26.
- Agarwal, A., Goswami, A., Vijayaraghavan, G.P., Srivastava, A., Kandwal, P., Nagaraja, U.B., Goel, V.K., Agarwal, A.K., Jayaswal, A., 2019. Quantitative Characteristics of Consecutive Lengthening Episodes in Early-onset Scoliosis (EOS) Patients with Dual Growth Rods. *Spine (Phila. Pa. 1976)*. 44, 397–403. <https://doi.org/10.1097/BRS.0000000000002835>.
- Agarwal, A., Jayaswal, A., Goel, V.K., Agarwal, A.K., 2018. Patient-specific Distraction Regimen to Avoid Growth-rod Failure. *Spine (Phila. Pa. 1976)*. 43, E221–E226.
- Akbarnia, B.A., Marks, D.S., Boachie-Adjei, O., Thompson, A.G., Asher, M.A., 2005. Dual growing rod technique for the treatment of progressive early-onset scoliosis: A multicenter study. *Spine (Phila. Pa. 1976)*. <https://doi.org/10.1097/01.brs.0000175190.08134.73>.
- Cahill, P.J., Marvil, S., Cuddihy, L., Schutt, C., Idema, J., Clements, D.H., Antonacci, M. D., Asghar, J., Samdani, A.F., Betz, R.R., 2010. Autofusion in the immature spine treated with growing rods. *Spine (Phila. Pa. 1976)*. 35, E1199–E1203. <https://doi.org/10.1097/BRS.0b013e3181e21b50>.
- Chazal, J., Tanguy, A., Bourges, M., Gaurel, G., Escande, G., Guillot, M., Vanneville, G., 1985. Biomechanical properties of spinal ligaments and a histological study of the supraspinal ligament in traction. *J. Biomech.* 18, 167–176.
- Cheung, J.P.Y., Bow, C., Samartzis, D., Kwan, K., Cheung, K.M.C., 2016. Frequent small distractions with a magnetically controlled growing rod for early-onset scoliosis and avoidance of the law of diminishing returns. *J. Orthop. Surg.* 24, 332–337.
- Cheung, K.M.C., Cheung, J.P.Y., Samartzis, D., Mak, K.C., Wong, Y.W., Cheung, W.Y., Akbarnia, B.A., Luk, K.D.K., 2012. Magnetically controlled growing rods for severe spinal curvature in young children: A prospective case series. *The Lancet* 379, 1967–1974. [https://doi.org/10.1016/S0140-6736\(12\)60112-3](https://doi.org/10.1016/S0140-6736(12)60112-3).
- Ching, R.P., Nuckley, D.J., Hertsted, S.M., Eck, M.P., Mann, F.A., Sun, E.A., 2001. Tensile Mechanics of the Developing Cervical Spine. *Stapp Car Crash J.* 45, 2001-P-375. <https://doi.org/10.4271/2001-22-0015>.
- DeWit, J.A., Cronin, D.S., 2012. Cervical spine segment finite element model for traumatic injury prediction. *J. Mech. Behav. Biomed. Mater.* 10, 138–150. <https://doi.org/10.1016/j.jmbm.2012.02.015>.
- Dibb, A.T., Nightingale, R.W., Luck, J.F., Carol Chancey, V., Fronheiser, L.E., Myers, B.S., 2009. Tension and combined tension-extension structural response and tolerance properties of the human male ligamentous cervical spine. *J. Biomech. Eng.* 131, 081008 <https://doi.org/10.1115/1.3127257>.
- Dong, L., Li, G., Mao, H., Marek, S., Yang, K.H., 2013. Development and validation of a 10-year-old child ligamentous cervical spine finite element model. *Ann. Biomed. Eng.* 41, 2538–2552. <https://doi.org/10.1007/s10439-013-0858-7>.
- Dreischarf, M., Zander, T., Shirazi-Adl, A., Puttlitz, C.M., Adam, C.J., Chen, C.S., Goel, V. K., Kiapour, A., Kim, Y.H., Labus, K.M., Little, J.P., Park, W.M., Wang, Y.H., Wilke, H.J., Rohlmann, A., Schmidt, H., 2014. Comparison of eight published static finite element models of the intact lumbar spine: Predictive power of models improves when combined together. *J. Biomech.* 47, 1757–1766.
- Duncan, J.M., 1874. Laboratory note: On the tensile strength of the fresh adult foetus. *Br. Med. J.* 2, 763. <https://doi.org/10.1136/bmj.2.729.763>.
- Dunn, H.K., Daniels, A.U., McBride, G.G., 1982. Intraoperative force measurements during correction of scoliosis. *Spine (Phila. Pa. 1976)*. 7, 448–455. <https://doi.org/10.1097/00007632-198209000-00008>.
- Elfstrom, G., Nachemson, A., 1973. Telemetry recordings of forces in the Harrington distraction rod: a method for increasing safety in the operative treatment of scoliosis patients. *Clin. Orthop. Relat. Res.* 93, 158–172. <https://doi.org/10.1097/00003086-197306000-00016>.
- FDA, 2019. Recommended Content and Format of Non-Clinical Bench Performance Testing Information in Premarket Submissions. Published online 2019. Accessed from: <https://www.fda.gov/media/113230/download>.
- FDA, 2016. Reporting of Computational Modeling Studies in Medical Device Submissions. Appendix II - Computational Solid Mechanics. Published online 2016. Accessed from: <https://www.fda.gov/media/87586/download>.
- Henaou, J., Labelle, H., Arnoux, P.J., Aubin, C.É., 2018. Biomechanical Simulation of Stresses and Strains Exerted on the Spinal Cord and Nerves During Scoliosis Correction Maneuvers. *Spine Deform* 6, 12–19. <https://doi.org/10.1016/j.jspd.2017.04.008>.
- Jebaseelan, D.D., Jebaraj, C., Yoganandan, N., Rajasekaran, S., Kanna, R.M., 2012. Sensitivity studies of pediatric material properties on juvenile lumbar spine responses using finite element analysis. *Med. Biol. Eng. Comput.* 50, 515–522.
- Kumaresan, S., Yoganandan, N., Pintar, F.A., Maiman, D.J., Kuppa, S., 2000. Biomechanical study of pediatric human cervical spine: A finite element approach. *J. Biomech. Eng.* 122, 60–71.

- Luck, J.F., Nightingale, R.W., Song, Y., Kait, J.R., Loyd, A.M., Myers, B.S., "Dale Bass, C. R., 2013. Tensile Failure Properties of the Perinatal, Neonatal, and Pediatric Cadaveric Cervical Spine. *Spine (Phila. Pa. 1976)*. 38, E1–E12. <https://doi.org/10.1097/BRS.0b013e3182793873>.
- Lemans, J.V.C., Wijdicks, S.P.J., Castelein, R.M., Kruyt, M.C., 2021. Spring Distraction System for Dynamic Growth Guidance of Early Onset Scoliosis: 2 Year Prospective Follow-up of 24 Patients. *Spine J.* 21, 671–681. <https://doi.org/10.1016/j.spinee.2020.11.007>.
- Moher, D., Liberati, A., Tetzlaff, J., Altman, D.G., 2009. Preferred reporting items for systematic reviews and meta-analyses: The PRISMA statement. *PLoS Med.* 6, e1000097.
- Myklebust, J.B., Pintar, F., Yoganandan, N., Cusick, J.F., Maiman, D., Myers, T.J., Sances, A., 1988. Tensile strength of spinal ligaments. *Spine (Phila. Pa. 1976)*. 13, 526–531.
- Naserkhaki, S., Arjmand, N., Shirazi-Adl, A., Farahmand, F., El-Rich, M., 2018. Effects of eight different ligament property datasets on biomechanics of a lumbar L4–L5 finite element model. *J. Biomech.* 70, 33–42.
- Noordeen, H.M., Shah, S.A., Elsebaie, H.B., Garrido, E., Farooq, N., Al Mukhtar, M., 2011. In vivo distraction force and length measurements of growing rods: Which factors influence the ability to lengthen? *Spine (Phila. Pa. 1976)*. 36, 2299–2303. <https://doi.org/10.1097/BRS.0b013e31821b8e16>.
- Nuckley, D.J., Linders, D.R., Ching, R.P., 2013. Developmental biomechanics of the human cervical spine. *J. Biomech.* 46, 1147–1154. <https://doi.org/10.1016/j.jbiomech.2013.01.005>.
- Ouyang, J., Zhu, Q., Zhao, W., Xu, Y., Chen, W., Zhong, S., 2005. Biomechanical Assessment of the Pediatric Cervical Spine Under Bending and Tensile Loading. *Spine (Phila. Pa. 1976)*. 30, E716–E723. <https://doi.org/10.1097/01.brs.0000192280.53831.70>.
- Pintar, F., Mayer, R., 2000. Child Neck Strength Characteristics Using An Animal Model. *Stapp Car Crash J.* 44, 2000-P-362.
- Poon, S., Spencer, H.T., Fayssoux, R.S., Sever, R., Cho, R.H., 2018. Maximal Force Generated by Magnetically Controlled Growing Rods Decreases With Rod Lengthening. *Spine Deform.* 6, 787–790. <https://doi.org/10.1016/j.jspd.2018.03.009>.
- Rushton, P.R.P., Smith, S.L., Forbes, L., Bowey, A.J., Gibson, M.J., Joyce, T.J., 2019. Force Testing of Explanted Magnetically Controlled Growing Rods. *Spine (Phila. Pa. 1976)*. 44, 233–239. <https://doi.org/10.1097/BRS.0000000000002806>.
- Slim, K., Nini, E., Forestier, D., Kwiatkowski, F., Panis, Y., Chipponi, J., 2003. Methodological index for non-randomized studies (Minors): Development and validation of a new instrument. *ANZ J. Surg.* 73, 712–716.
- Teli, M., Grava, G., Solomon, V., Andreoletti, G., Grismondi, E., Meswania, J., 2012. Measurement of forces generated during distraction of growingrods in early onset scoliosis. *World J. Orthop.* 3, 15–19. <https://doi.org/10.5312/wjo.v3.i2.15>.
- Waugh, T.R., 1966. Intravital measurements during instrumental correction of idiopathic scoliosis. *Acta Orthop. Scand.* 37, 1–87. <https://doi.org/10.3109/ort.1966.37.suppl-93.01>.
- Wijdicks, S.P.J., Lemans, J.V.C., Verkerke, G.J., Noordmans, H.J., Castelein, R.M., Kruyt, M.C., 2021. The potential of spring distraction to dynamically correct complex spinal deformities in the growing child. *Eur. Spine J.* 30, 714–723. <https://doi.org/10.1007/s00586-020-06612-3>.
- Williams IV, J.T., Southerland, S.S., Souza, J., Calcutt, A.F., Cartledge, R.G., 1999. Cells isolated from adult human skeletal muscle capable of differentiating into multiple mesodermal phenotypes. *Am. Surg.* 65, 22.
- Yang, C., Wang, H., Zheng, Z., Zhang, Z., Wang, J., Liu, H., Kim, Y.J., Cho, S., 2017. Halo-gravity traction in the treatment of severe spinal deformity: a systematic review and meta-analysis. *Eur. Spine J.* 26, 1810–1816. <https://doi.org/10.1007/s00586-016-4848-y>.
- Yankey, K.P., Duah, H.O., Sacramento-Domínguez, C., Tutu, H.O., Owiredo, M.A., Mahmud, R., Wulff, I., Ofori-Amankwah, G., Akoto, H., Boachie-Adjei, O., 2021. The Effect of Prolonged Pre-Operative Halo Gravity Traction for Severe Spinal Deformities on the Cervical Spine Radiographs. *Glob. Spine J.* 219256822199864 <https://doi.org/10.1177/2192568221998644>.
- Yoganandan, N., Kumaresan, S., Pintar, F.A., 2001. Biomechanics of the cervical spine. Part 2. Cervical spine soft tissue responses and biomechanical modeling. *Clin. Biomech.* 16, 1–27.
- Yoganandan, N., Pintar, F., Sances, A., Maiman, D., Myklebust, J., Harris, G., Ray, G., 1988. Biomechanical investigations of the human thoracolumbar spine. *SAE Tech. Pap.* 881331, 676–684 <https://doi.org/https://doi.org/10.4271/881331>.
- Yoganandan, N., Pintar, F.A., Kumaresan, S., Gennarelli, T.A., 2000. Pediatric and small female neck injury scale factors and tolerance based on human spine biomechanical characteristics. *IRCOBI Conference. Montpellier* 21–23.
- Yoganandan, N., Pintar, F.A., Maiman, D.J., Cusick, J.F., Sances, A., Walsh, P.R., 1996. Human head-neck biomechanics under axial tension. *Med. Eng. Phys.* 18, 289–294.